Effect of Surface Hydrophobicity on the Conformational Changes of Adsorbed Fibrinogen[1]

DONGHAO R. LU AND KINAM PARK[2]

Purdue University, School of Pharmacy, West Lafayette, Indiana 47907

The extent of conformational changes of fibrinogen adsorbed on germanium, poly(hydroxyethyl methacrylate) (poly(HEMA), Biomer, and polystyrene surfaces was studied using Fourier transform infrared spectroscopy (FTIR) coupled with attenuated total reflectance (ATR) optics. The contact angles of water on the solid surfaces were 19.3°, 35.5°, 37.6°, and 90.5°, respectively. The adsorption kinetics of fibrinogen from 1 mg/ml solution showed that the amount of adsorbed fibrinogen increased as the surface became more hydrophobic. The spectra of fibrinogen in the bulk solution and of fibrinogen tightly adsorbed on germanium, poly(HEMA), Biomer, and polystyrene surfaces were treated using Fourier self-deconvolution and the synthetic single-peak fitting techniques to resolve the overlapped peaks in the amide I and II regions. It was found that some α-helical structures were changed into the unordered structures and the content of β-turns was increased upon the protein adsorption. A weighted-peak shift method was used to examine the extent of the protein conformational changes upon adsorption on hydrophobic and hydrophilic surfaces. The results indicated that the adsorbed fibrinogen underwent a larger degree of conformational changes as the surface hydrophobicity increased. © 1991 Academic Press, Inc.

INTRODUCTION

Because of the importance of protein adsorption in the biomedical area, research on the interfacial behavior of proteins has been carried out extensively. Much attention has been paid to the conformational changes of proteins adsorbed on solid surfaces due to the importance of protein conformation in the bioactivity of the adsorbed proteins (1–5). For example, the conformational changes of fibrinogen adsorbed on solid surfaces are thought to be responsible for the platelet adhesion to the surface, since the intact fibrinogen in the bulk solution does not interact with platelets under the same conditions (6). The Fourier transform infrared spectroscopy coupled with attenuated total reflectance optics (FTIR-ATR) has been widely used for its ca-

pabilities of generating reproductible IR spectra of proteins on solid surfaces and characterizing biological samples on the basis of intrinsic spectral features (7).

It is generally accepted that the interaction between a protein and a surface increases with increasing hydrophobicity of either the surface or the protein (8, 9). It is expected that as the protein–surface interaction increases, the conformational changes of the adsorbed protein occur to a larger extent. To investigate such a relationship in more detail, we have examined the conformational changes of fibrinogen adsorbed on germanium, poly(hydroxyethyl methacrylate) (poly(HEMA)), Biomer, and polystyrene using FTIR-ATR techniques. Fibrinogen adsorption onto germanium and polymer surfaces has been studied extensively using FTIR-ATR. Most studies, however, have dealt with the kinetics of fibrinogen adsorption and the relative amount of adsorbed fibrinogen (3, 10–14). Conformational changes of fibrinogen on polyure-

271

thane surfaces with a different content of polyether segments were investigated by Stupp *et al.* (15). In our study, conformational changes of adsorbed fibrinogen were examined in relation to the surface hydrophobicity. Fourier self-deconvolution (FSD) was employed to resolve the intrinsically overlapped peaks in the amide I ($1700-1600$ cm^{-1}) and amide II ($1600-1480$ cm^{-1}) regions. A synthetic single-peak fitting technique was used along with the FSD method for the single-peak generation which was established by Kauppinen *et al.* (16). The extent of protein conformational changes was examined by calculating the sum of the shifts of individual peaks using a weighted-peak shift method. The results of our study indicate that the extent of the conformational changes for the adsorbed fibrinogen is related to the surface hydrophobicity.

MATERIALS AND METHODS

Attenuated Total Reflectance Apparatus

The Contact Sampler (Spectra Tech Inc., Stamford, CT), a horizontal internal reflectance accessory with a gripper, was modified to mount a single channel flow cell. The configuration of the Contact Sampler and the flow cell is shown in Fig. 1. The inner dimension of the flow cell was approximately 0.1 cm deep, 1 cm wide, and 7 cm long, and the space was provided with a silicone rubber gasket (polydimethylsiloxane, Thoratec Lab, Berkeley, CA). Only the upper side of the ATR crystal

FIG. 1. Schematic description of the flow cell setup.

was used for protein adsorption. The lid of the flow cell was made of aluminum and the flow cell was tightly held on the Contact Sampler by the gripper. The utilization of the flow cell eliminated surface–air contact and allowed introduction of protein solutions without opening the FTIR compartment. The ATR crystal, which was permanently held in a metal plate, had an incident angle of 45°. A germanium crystal was used as the ATR optic element.

Preparation of Polymer Films on Germanium Surface

Polystyrene (Aldrich, Milwaukee, WI), poly(HEMA) (Aldrich), and Biomer (segmented polyether polyurethane, Ethicon, Somerville, NJ) were used for preparing polymer films on an ATR crystal. Polystyrene was dissolved in toluene, poly(HEMA) in *N,N*-dimethylformamide (DMF), and Biomer in *N,N*-dimethylacetamide (DMA) to make polymer solutions.

The germanium ATR crystal was soaked in a 5% SDS detergent solution for 30 min, rubbed with lens cloth tissue (Bel-Art Products, Pequannock, NJ) in the presence of SDS detergent, rinsed with copious amount of distilled deionized water (Nanopure, Barnsted), washed with toluene twice, and finally cleaned again with distilled deionized water. Five-milliliter drops of the polymer solution were applied on the crystal for 3 min to form a polymer solution layer. The crystal plate was tilted to drain the solution from the edge using paper towels. A thin film of the polymer solution remained and was air-dried for 4 h before use.

The contact angles of water droplets on the germanium, poly(HEMA), Biomer, and polystyrene surfaces were measured using a goniometer (Rame–Hart Inc., Mountain Lakes, NJ). Eight readings on different parts of each surface were averaged.

Although no attempt was made to estimate the thickness of the coated polymer film, several protein adsorption experiments were conducted to ensure that adsorbed protein molecules were detected by the infrared eva-
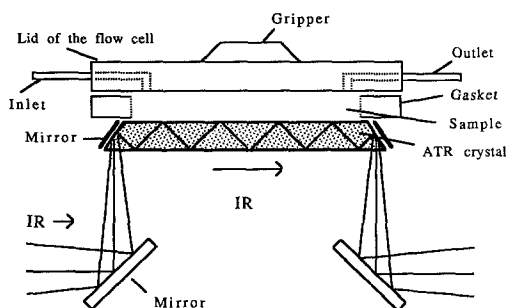
nescent wave. The polymer concentration was varied from 0.05 to 1% (w/v) to change the thickness of the polymer coating. The spectrum of the adsorbed protein on the polymer-coated ATR crystal was used to determine the appropriate polymer concentration which was related to the thickness of the polymer coating. The polymer concentration of 0.1% (w/v) was found to be adequate to prepare the polymer coating on the germanium crystal.

Protein Preparation

Human fibrinogen obtained from Sigma (Type I, clottability over 90%) was further purified using the Laki method (17). During the purification 0.1 M ϵ-aminocaproic acid was used to prevent the activation of plasminogen. $BaSO_4$ (40 g per gram of fibrinogen) was added to the fibrinogen solution to remove prothrombin and related clotting factors (18). The fibrinogen solution was run through a gelatin column equilibrated with phosphate-buffered saline (PBS, pH 7.4) without divalent cations to remove fibronectin. The purified fibrinogen was at least 97% clottable. The fibrinogen was then reprecipitated by saturated ammonium sulfate (about one-third of the volume) and redissolved in the PBS solution. Clear supernate obtained after centrifugation was dialyzed in PBS solution for 24 h at 4°C. The concentration of the purified fibrinogen was measured by UV absorbance at 280 nm (19) and the aliquots of fibrinogen solution were stored at −70°C.

FTIR Experiments for Adsorbed Fibrinogen and Fibrinogen in PBS Solution

The IR spectra were acquired using a Nicolet 20SXc Fourier transform infrared system (Nicolet, Madison, WI) equipped with a liquid-nitrogen-cooled mercury–cardium–telluride (MCT) detector. Data were collected at 8 cm⁻¹ resolution. For protein adsorption experiments, the background spectrum of the ATR apparatus (with or without the polymer coating) was obtained. PBS solution was introduced into the cell and the reference spec-

trum was obtained after 30 min of equilibrium. The buffer was then replaced by the fibrinogen solution (1 mg/ml) and sample spectra were taken during a 1.5-h period in the static state. A macro computer program was written to control the scanning intervals. The spectra were collected with six coadded scans in the beginning and the number of coadded scans became larger later. The spectra were collected in interferograms during the experiment to avoid the time required for Fourier transform processing, which was performed after the experiment. After 1.5 h of protein adsorption, the cell was washed with 6 ml of PBS solution and the FTIR spectrum of tightly adsorbed fibrinogen was taken.

The transmission FTIR spectrum of fibrinogen in PBS solution was obtained using a demountable path-length liquid sampling cell (Spectra Tech Inc.) with CaF_2 windows and a 15-μm spacer. One thousand coadded scans were taken for each spectrum background (empty cell), reference (PBS solution), and sample (1 mg/ml fibrinogen in PBS solution).

All spectra in interferograms were Fourier transformed. The single-beam reference and sample spectra were then set in a 1:1 ratio against the background spectrum to obtain the spectra of polymer/PBS solution and fibrinogen/polymer/PBS solution. The polymer/PBS spectrum was properly subtracted from the fibrinogen/polymer/PBS spectrum by an interactive change of subtraction factor (about 0.95 to 1.00) to provide a straight-line baseline from 1400 to 1000 cm⁻¹. Water vapor subtraction and baseline correction between 2000 and 1000 cm⁻¹ were performed before the quantitative measurement and the spectrum deconvolution.

The quantitative measurement of adsorbed protein was accomplished by integrating the amide II band above the baseline from 1590 to 1495 cm⁻¹ (10, 20). All spectra were the coadded spectra from two duplicate experiments for the adsorption kinetic study. The spectra for tightly adsorbed fibrinogen from two duplicate experiments with a total of 2000 scans were coadded and used for the spectrum

deconvolution. The deconvolution was performed in the amide I and II regions with full width at half-maximum (FWHM) of 34 cm^{-1} for the amide I region (1700 to 1600 cm^{-1}) and FWHM of 26 cm^{-1} for the amide II region (1600 to 1480 cm^{-1}). The width deflation factor was 2.3 for both regions (4). The Gaussian apodization function was used for the synthetic single-peak fitting (21). The deconvolution and the synthetic single-peak fitting were accomplished using the FOCAS computer program from the Nicolet Instrument Corp. During the execution of the program, the spectrum was deconvolved and the peak position of each overlapped peak was resolved. The peak positions were then used in the synthetic single-peak fitting to generate overlapped peaks.

Weighted-Peak Shift Method

All the peak shifts were considered to address the extent of the conformational changes of fibrinogen adsorbed on solid surfaces. The direction of the shift for each peak was not considered because the conformational changes might cause the shift in either direction for each peak. The peak with higher peak intensity is expected to have a greater contribution to the conformational changes than the one with lower peak intensity, if both peaks have the same extent of shift. Therefore, the peak shift for each peak was weighted according to the peak intensity. All the weighted-peak shifts were then added together to determine the extent of conformational changes.

The sum of the weighted-peak shifts was calculated as follows. The differences in the single-peak positions between the spectra of fibrinogen on the surfaces and in the bulk solution (i.e., the reference spectrum of unadsorbed fibrinogen) were taken as unweighted-peak shifts (ΔS_i). The peak shift was then weighted by the intensity of each peak in the reference spectrum. All weighted-peak shifts were added together to calculate E_S, sum of the weighted-peak shifts, using

$$E_S = \sum_{\text{peak } i} f_i \Delta S_i, \qquad [1]$$

where f_i is the weighting factor based on the intensity in the reference spectrum. The E_S was used to examine the extent of conformational changes of fibrinogen upon adsorption.

RESULTS

The contact angles of water on the germanium, poly(HEMA), Biomer, and polystyrene surfaces are listed in Table I. Of the four surfaces, polystyrene was the most hydrophobic and germanium was the most hydrophilic. Poly(HEMA) and Biomer were intermediate.

The adsorption kinetics of fibrinogen on germanium, poly(HEMA), Biomer, and polystyrene surfaces from 1 mg/ml fibrinogen solution are shown in Fig. 2. The quantitative measurement was made by integrating the amide II band in each spectrum with different adsorption times. The spectra from two duplicate experiments were coadded before the integration. Therefore, no error bars are shown in the figure. The data for the early adsorption time were approximate since the number of coadded scans was too low. The accuracy of the measurements was improved later due to the larger number of coadded scans. At 10 min of adsorption, the number of coadded scans was increased to 400. Since there was unadsorbed fibrinogen in the bulk solution within the field of the evanescent wave, the spectra before the removal of bulk fibrinogen included the information for both the adsorbed and the unadsorbed fibrinogen. After the PBS washing at 90 min, fibrinogen in the bulk solution and some loosely adsorbed fibrinogen were elim-

TABLE I

The Contact Angles of Water Droplets on Solid Surfaces

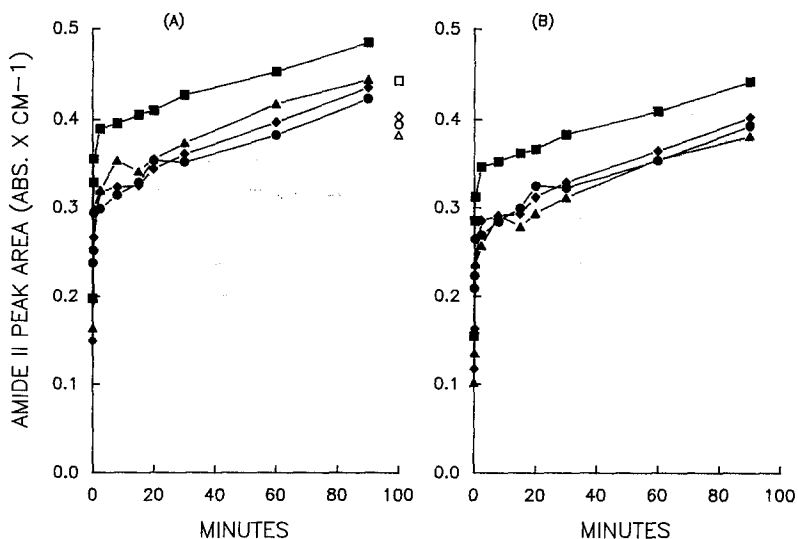| Solid surface	Contact angle
Germanium	19.25 ± 2.12*
Poly(HEMA)	35.50 ± 2.51
Biomer	37.63 ± 1.46
Polystyrene	90.50 ± 3.16

* Average $\pm$ SD.

FIG. 2. The adsorption kinetics of fibrinogen on solid surfaces. (A) The absorbance in the presence of bulk fibrinogen; (B) absorbance for tightly adsorbed fibrinogen only. ■, Polystyrene; ♦, Biomer; ●, poly(HEMA); and ▲, germanium. The open symbols in (A) represent the absorbance values after washing the flow cell with PBS.

inated and only tightly adsorbed fibrinogen remained. The spectrum for tightly adsorbed fibrinogen remaining on the surface was obtained with a total of 2000 coadded scans. The open symbols in Fig. 2A represent the quantitative measurements for the tightly adsorbed fibrinogen. The differences in the measurements before and after the PBS washing were 0.062, 0.029, 0.032, and 0.043 units (absorbance $\times$ cm^{-1}) for fibrinogen adsorption on germanium, poly(HEMA), Biomer, and polystyrene surfaces, respectively. It may be reasonable to consider that the influence of unadsorbed fibrinogen in bulk solution was approximately constant. Therefore, the quantitative measurement for tightly adsorbed fibrinogen on the solid surfaces with different adsorption times can be calculated by subtracting the difference. Figure 2B represents the calculated adsorption kinetics for tightly adsorbed fibrinogen. In Fig. 2A it is seen that the amount of fibrinogen on germanium was higher than that on poly(HEMA) and Biomer but the result was reversed in Fig. 2B. This is most likely due to the polymer coatings which reduced the range of the evanescent wave. The

results for tightly adsorbed fibrinogen indicate that the amount of adsorbed fibrinogen increases when the surface hydrophobicity increases.

Figure 3 shows the spectra of fibrinogen in PBS solution and fibrinogen tightly adsorbed on germanium, poly(HEMA), Biomer, and polystyrene surfaces. It is apparent that the amide I bands of adsorbed fibrinogen on the solid surfaces are wider than those of fibrinogen in PBS solution. The same observation was made for albumin adsorbed on other surfaces (4). There is a unique shoulder near 1625 cm^{-1} in the spectrum of bulk fibrinogen. A similar shoulder was also found in the deconvolved spectrum of bulk albumin (4). The spectra for fibrinogen in PBS solution and for the tightly adsorbed fibrinogen on the solid surfaces were treated using Fourier self-deconvolution and synthetic single-peak fitting techniques. The resolved overlapped single peaks in amide I and II regions for fibrinogen in PBS solution and fibrinogen adsorbed on germanium, poly(HEMA), Biomer, and polystyrene surfaces are shown in Fig. 4. The single peaks have a symmetric shape and the
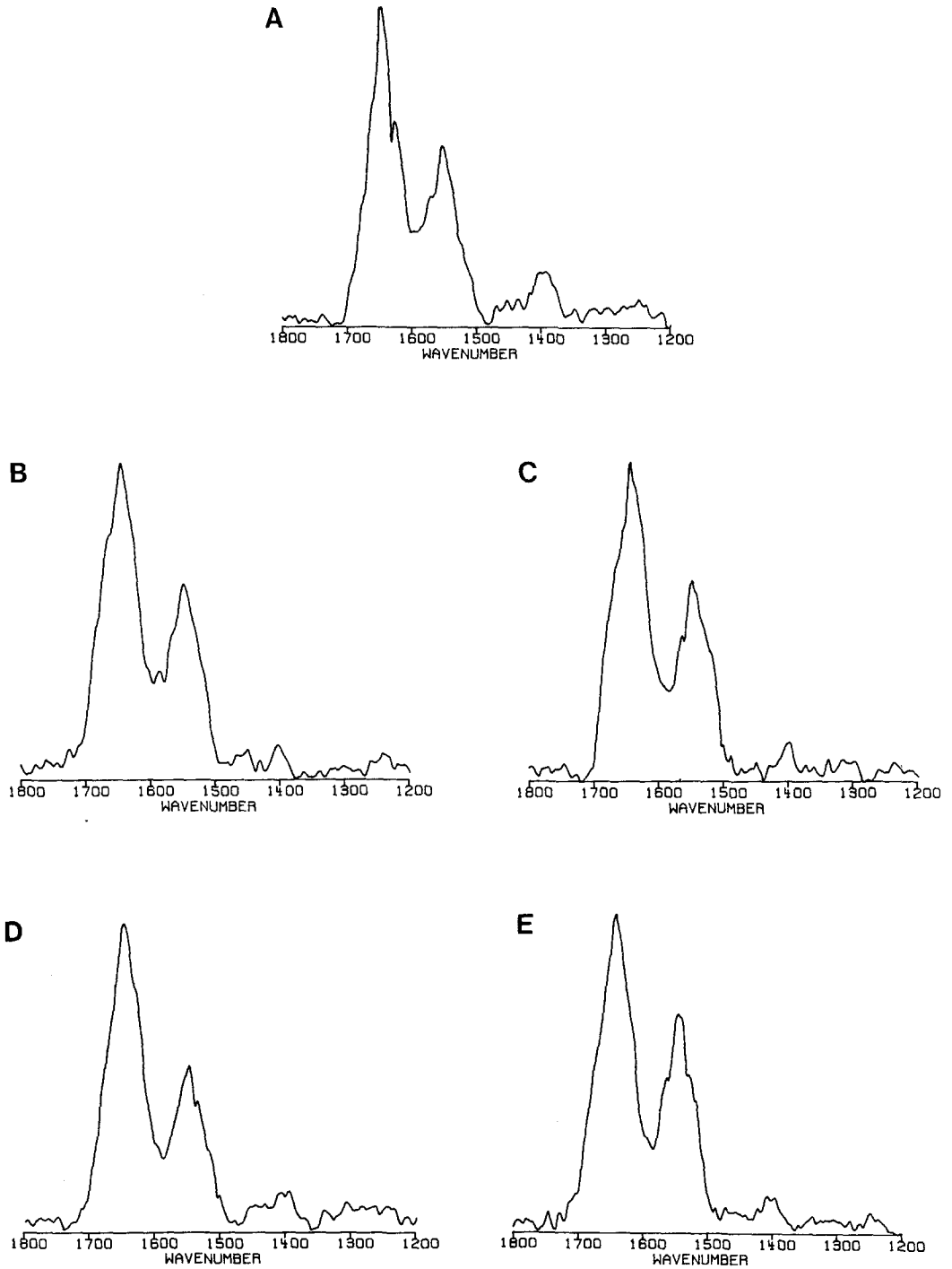
FIG. 3. The FTIR spectra of fibrinogen in PBS buffer (A) and of fibrinogen tightly adsorbed on germanium (B), poly(HEMA) (C), Biomer (D), and polystyrene (E).
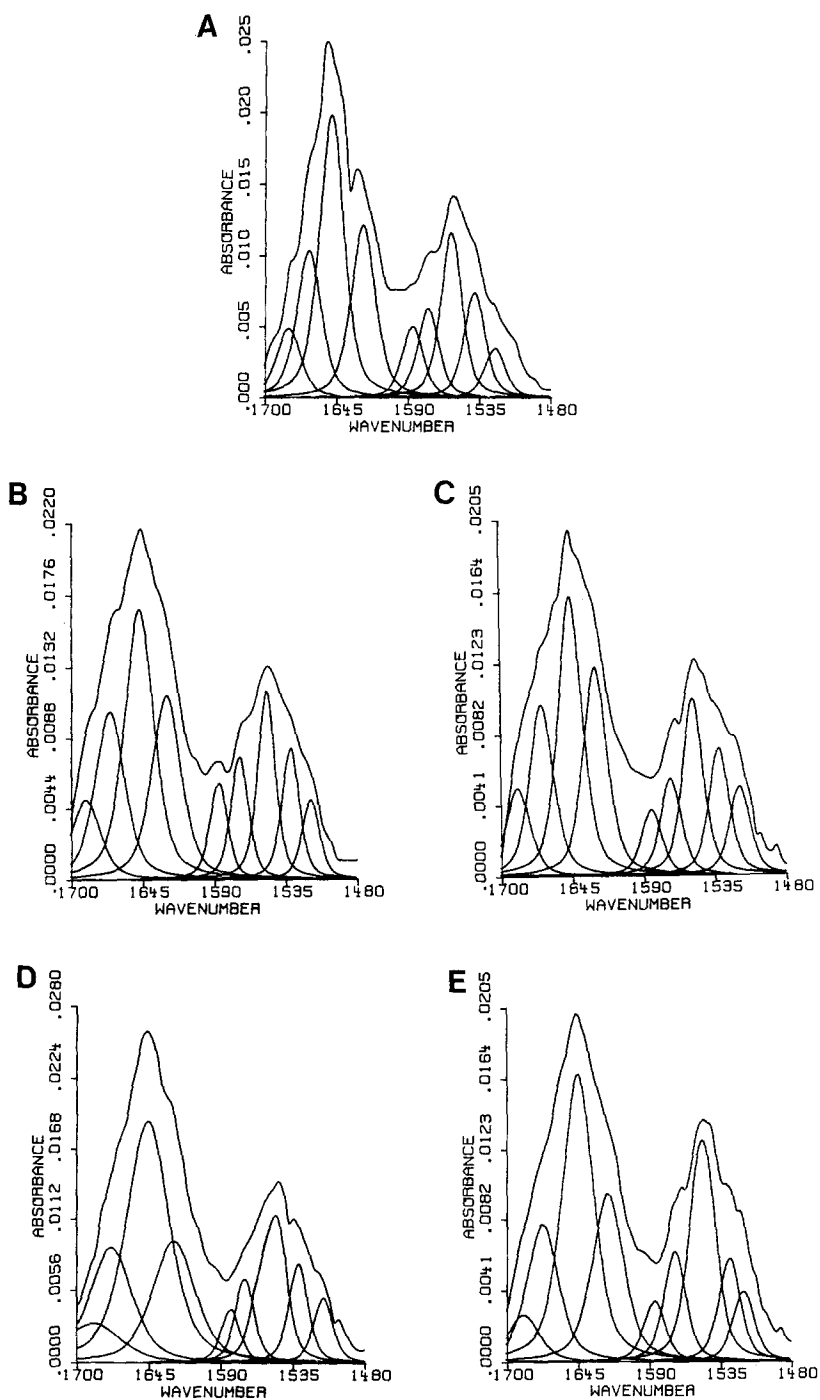
FIG. 4. The FTIR spectra (in the amide I and II regions) of fibrinogen in PBS buffer (A) and of fibrinogen tightly adsorbed on germanium (B), poly(HEMA) (C), Biomer (D), and polystyrene (E). The original spectra are also plotted with the resolved overlapped single peaks for comparison.

LU AND PARK

TABLE II

Peak Position and Peak Intensity (in Parentheses) for the Deconvolved Spectra in the Amide I Region

Unadsorbed	1682	1666	1650	1624
	(0.0049)	(0.0104)	(0.0199)	(0.0122)
On germanium	1689	1671	1648	1627
	(0.0049)	(0.0105)	(0.0168)	(0.0115)
On poly(HEMA)	1687	1669	1646	1627
	(0.0051)	(0.0099)	(0.0162)	(0.0121)
On biomer	1687	1674	1646	1626
	(0.0030)	(0.0090)	(0.0191)	(0.0095)
On polystyrene	1687	1673	1645	1622
	(0.0027)	(0.0079)	(0.0167)	(0.0097)

summation of the single peaks makes up the original spectrum. For all the spectra in Fig. 4, the amide I and II regions were composed of four and five single peaks, respectively. Both in the amide I and in the amide II regions, there is a main peak (the peak with the highest intensity) which contributes the most to the original spectrum. The peak positions and the peak intensities in the amide I and amide II regions are listed in Tables II and III, respectively. The main peaks in the amide I region were averaged at 1647 cm^{-1} (Table II) and in the amide II region at 1552 cm^{-1} (Table III). Compared with the peak positions in the spectrum of fibrinogen in PBS solution, the main peaks (both in amide I and in amide II regions) in the spectra of adsorbed fibrinogen were all shifted to the direction of lower wavenumber. In the amide I region, the shift of the main peak became greater as the surface hydrophobicity increases as shown in Table II. In the

amide II region, all the peaks tended to shift to the direction of lower wavenumber. In the amide I region, however, the peak shift occurred in both directions. The peak near 1686 and 1671 cm^{-1} shifted to the direction of higher wavenumber, while no tendency was observed for the peak near 1625 cm^{-1}.

Since it was known that the peak shift was related to the conformational changes of the adsorbed protein (4), the effect of surface hydrophobicity on the extent of peak shift was examined. All peak shifts were weighted according to intensity differences in the reference spectrum (the one for the bulk fibrinogen). The weighting factor (f_i) was set to be 100% for the first peak (at 1682 cm^{-1}). The weighting factor for the rest of the peaks were calculated as the ratio of the intensity of each peak to the intensity of the peak at 1682 cm^{-1}. The values for the weighting factors are listed in Table IV. The calculated E_S for the adsorp-

TABLE III

Peak Position and Peak Intensity (in Parentheses) for the Deconvolved Spectra in the Amide II Region

Unadsorbed	1587	1575	1557	1539	1523
	(0.0051)	(0.0063)	(0.0117)	(0.0074)	(0.0035)
On germanium	1587	1571	1550	1532	1516
	(0.0060)	(0.0077)	(0.0117)	(0.0082)	(0.0049)
On poly(HEMA)	1585	1570	1552	1532	1516
	(0.0038)	(0.0056)	(0.0103)	(0.0073)	(0.0051)
On biomer	1585	1572	1551	1531	1513
	(0.0042)	(0.0063)	(0.0113)	(0.0077)	(0.0057)
On polystyrene	1586	1570	1551	1528	1517
	(0.0035)	(0.0063)	(0.0127)	(0.0059)	(0.0040)

TABLE IV

The Weighting Factor (%) for the Four Peaks in the Amide I Region and the Five Peaks in the Amide II Region

Amide I peaks					
Single-peak (cm^{-1})		1682	1666	1650	1624
Weighting factor		100	212	406	249
Amide II peaks					
Single-peak (cm^{-1})	1587	1575	1557	1539	1523
Weighting factor	104	129	239	151	71

tion of fibrinogen on germanium, poly-(HEMA), Biomer, and polystyrene surfaces are listed in Table V. There is only a slight difference in E_S values between germanium and poly(HEMA). The values for Biomer and polystyrene, however, are much larger than the value for germanium. It appears that the extent of conformational changes of fibrinogen on the solid surfaces generally increases as the surface hydrophobicity becomes greater.

DISCUSSION

Within the IR spectrum of protein, amide I, II, and III bands, which involve coupled C=O stretching. C–N stretching, and N–H bending of the peptide groups, are particularly interesting. Two theoretical approaches to the analysis of the protein spectrum for the conformational study have been suggested. The first one was a perturbation treatment applied by Miyazawa (22). A weakly coupled oscillator model was used to treat the amide I or II vibrations of a polypeptide chain. The approach was refined later by Krimm (23). The standard structures of α-helix, parallel-chain,

TABLE V

The Sum of the Weighted-Peak Shifts, E_S, for Adsorption of Fibrinogen on the Solid Surfaces

Surface	E_s
Germanium crystal	70.62
Poly(HEMA)	71.09
Biomer	82.65
Polystyrene	87.82

and antiparallel-chain pleated sheets and the polar-chain pleated sheet were studied. The frequencies for the standard structure were calculated in detail (24). The second approach was a comparative assignment for the α-helix, β-structure, turns and bends, and unordered structure according to an FTIR deconvolution study of a series of proteins with known secondary structures (3, 25). In our study, we have applied the second approach for the peak assignment because of the use of a deconvolved spectrum. Due to the low signal-to-noise ratio, we were not able to make spectrum deconvolution from the amide III region. Therefore, it was not considered in our study.

The goal of our study was to examine the effect of surface hydrophobicity on the conformational changes of adsorbed fibrinogen by the FTIR-ATR technique. The issue was addressed by Pitt et al., who examined conformational changes of fibrinogen (2). In their study, the adsorption of fibronectin on surfaces of polyurethane ureas with different hydrophobicities was examined. The contact angles of water on the polymer surfaces used in their study were 35°, 38°, and 59°, respectively. From the differences in amide I absorbance at 1669 cm^{-1} and the COOH peak at 1720 cm^{-1}, they found that the extent of spectral changes of adsorbed fibronectin was greater on the hydrophobic surface than on the hydrophilic surface. In our study, a greater range of surface hydrophobicities was chosen. As indicated in Table I, the contact angles of water on the germanium, poly(HEMA), Biomer, and polystyrene surfaces ranged from 19.3° to 90.5°.

The effect of surface hydrophobicity on the conformational changes was examined using a weighted-peak shift method, which was based on the results of the spectrum deconvolution and synthetic single-peak fitting.

Figure 4A shows the synthetic single peaks in the amide I and II regions for fibrinogen in PBS solution. There are four single peaks in the amide I region and five single peaks in the amide II region. We followed the work of Byler and Susi for the peak assignment in the amide I region (25). The average peak assignments, as listed in Table VI, were obtained from the study of 17 globular proteins with known secondary structures. According to the peak assignments, the peaks at 1682 and 1666 cm^{-1} were attributed to the structures of turns and bends. The peak at 1650 cm^{-1} was attributed to the mixed α-helical and unordered structures since the peak was located between the assignments for α-helix at 1654 cm^{-1} and unordered structures at 1645 cm^{-1}. The peak at 1624 cm^{-1} was attributed to the β-sheet. Figures 4B–4E show the corresponding synthetic single peaks in amide I and II regions for adsorbed fibrinogen. Several peak shifts are apparent upon the protein adsorption on solid surfaces. For all four spectra, both peaks for

TABLE VI

Deconvolved Amide I Frequencies (cm^{-1}) and Assignments Obtained from the Study of 17 Globular Proteins[a]

Structure segment	Frequency
β-sheet	
Frequency 1	1637
Frequency 2	1631
Frequency 3	1624
Frequency 4	1675
α-helix	1654
Unordered	1645
Turns and bends	
Frequency 1	1663
Frequency 2	1670
Frequency 3	1683
Frequency 4	1688
Frequency 5	1694

[a] The values were taken from Ref. (25).

the structures of turns and bends (near 1682 and 1666 cm^{-1}) are shifted to the direction of higher wavenumber, averaged at 1688 and 1672 cm^{-1}, respectively. Since the frequencies of 1688 and 1670 cm^{-1} are also known for the turns and bends, it appears that the adsorption induces conformational changes between the different modes of the turns and bends. For both peaks, there is no apparent trend to correlate the extent of the peak shift to the surface hydrophobicity. The peaks corresponding to the α-helix and unordered structures are found to shift to the direction of lower wavenumber, which is closer to the frequency for the unordered structure. Therefore, it is likely that upon adsorption, some of the α-helical structure was broken and changed into the unordered structure. It is noted that this peak is the main peak in the amide I region and that it has the highest intensity. The shift of this peak is thus expected to contribute the most to the conformational changes upon the protein adsorption. It can be seen that the extent of the shift of this peak correlates with the surface hydrophobicity. The higher the surface hydrophobicity, the greater the peak shift. The result of decreasing α-helical content upon protein adsorption is consistent with other works involving other proteins. It was found that the adsorption of albumin on polyetherurethane or soft contact lens surfaces reduced the α-helical content in the protein (1, 2). For the peaks near 1624 cm^{-1}, peak shifts occurred in both directions.

The assignments of all peaks in the amide II region were not made due to the lack of references for the peak assignments. One of the peaks, however, deserves further discussion. The peak at 1531 cm^{-1} was assigned to the generation of β-turns during the opening of the polypeptide chain (4, 26). In our study, there was a peak at 1539 cm^{-1} for the bulk fibrinogen. The peaks shifted to the direction of lower wavenumber, averaged at 1531 cm^{-1}. These peak shifts indicated a gain of β-turns upon the fibrinogen adsorption. The result is similar to those obtained from the studies of other proteins (4, 26).

The extent of the conformational changes of fibrinogen adsorbed on the four surfaces was examined using the weighted-peak shift method. Table V indicates that the solid surface with a higher hydrophobicity gives a greater value for the sum of the weighted-peak shifts. Since the analysis of the conformational changes by the weighted-peak shift method is new, it is difficult to conclude at this point whether this method quantitates the absolute magnitude of protein conformational changes. The sum of the weighted-peak shifts, however, is expected to correlate with the relative extent of conformational changes. Using the total internal reflection fluorescence technique, Iwamoto et al. also found that fibronectin experienced greater conformational changes on a more hydrophobic silica surface (27). When protein adsorbs on a solid surface with high hydrophobicity, the hydrophobic core is likely to become exposed to the surface due to the hydrophobic interaction. Thus, the larger conformational changes on more hydrophobic surfaces are understandable.

Since the peak shifts in the FTIR spectrum are related to conformational changes of adsorbed protein on the solid surface, the weighted-peak shift method can be used to examine the extent of conformational changes upon protein adsorption. The sum of the weighted-peak shifts reflects all the information in amide I and II regions and, therefore, generates an overall picture of the conformational changes.

REFERENCES

1. Castillo, E. J., Koenig, J. L., Anderson, J. M., and Lo, J., *Biomaterials* **5**, 319 (1984).
2. Pitt, W. G., Spiegelberg, S. H., and Cooper, S. L., *in* "Proteins at Interfaces: Physicochemical and Biochemical Studies" (J. L. Brash and T. A. Horbett, Eds.), p. 324. American Chemical Society, Washington, DC, 1987.
3. Jakobsen, R. J., and Wasacz, F. M., *in* "Proteins at Interfaces: Physicochemical and Biochemical Studies" (J. L. Brash and T. A. Horbett, Eds.), p. 339. American Chemical Society, Washington, DC, 1987.
4. Lenk, T. J., Ratner, B. D., Gendreau, R. M., and Chittur, K. K., *J. Biomed. Mater. Res.* **23**, 549 (1989).
5. Kato, K., Matsui, T., and Tanaka, S., *Appl. Spectrosc.* **41**, 861 (1987).
6. Tomikawa, M., Iwamoto, M., Olsson, P., Soderman, S., and Blomback, B., *Thromb. Res.* **19**, 869 (1980).
7. Knutson, K., and Lyman, D. L., *Org. Coat. Plast. Chem.* **42**, 621 (1980).
8. Lyklema, J., *Colloids Surf.* **10**, 33 (1984).
9. Andrade, J. D., and Hlady, V., *Adv. Polym. Sci.* **79**, 1 (1986).
10. Gendreau, R. M., Leininger, R. I., Winters, S., and Jakobsen, R. J., *in* "Biomaterials: Interfacial Phenomena and Applications" (S. L. Cooper and N. A. Peppas, Eds.), p. 371. American Chemical Society, Washington, DC, 1982.
11. Jakobsen, R. J., Brown, L. L., Winters, S., and Gendreau, R. M., *J. Biomed. Mater. Res.* **16**, 199 (1983).
12. Kellner, R., and Gotzinger, G., *Makrochimica Acta* **2**, 61 (1984).
13. Pitt, W. G., Park, K., and Cooper, S. L., *J. Colloid Interface Sci.* **111**, 343 (1986).
14. Chittur, K. K., Fink, D. J., Leininger, R. I., and Hutson, T. B., *J. Colloid Interface Sci.* **11**, 419 (1986).
15. Stupp, S. L., Kauffman, J. W., and Carr, S. H., *J. Biomed. Mater. Res.* **11**, 237 (1977).
16. Kauppinen, J. K., Moffatt, D. J., Mantsch, H. H., and Cameron, D. G., *Appl. Spectrosc.* **35**, 271 (1981).
17. Laki, K., *Arch. Biochem. Biophys.* **32**, 317 (1951).
18. Walker, L., and Catlin, A., *Thromb. Diath. Haemorrh.* **26**, 99 (1971).
19. Park, K., Mao, F. W., and Park, H., *Biomaterials* **11**, 24 (1990).
20. Pitt, W. G., and Cooper, S. L., *J. Biomed. Mater. Res.* **22**, 359 (1988).
21. James, D. I., Maddams, W. F., and Tooke, P. B., *Appl. Spectrosc.* **41**, 1362 (1987).
22. Miyazawa, T., *J. Chem. Phys.* **32**, 1647 (1960).
23. Krimm, S., *J. Mol. Biol.* **4**, 528 (1962).
24. Dwivedi, A. M., and Krimm, S., *Macromolecules* **15**, 186 (1982).
25. Byler, D. M., and Susi, H., *Biopolymers* **25**, 469 (1986).
26. Dev, S. B., and Rha, C. K., *J. Biomol. Struct. and Dyn.*, **2**, 431 (1984).
27. Iwamoto, G. K., Winterton, L. C., Stoker, R. S., van Wagenen, R. A., Andrade, J. D., and Mosher, D. F., *J. Colloid Interface Sci.* **106**, 459 (1985).